SCIENTIFIC REPORTS

OPEN

SUBJECT AREAS:
NANOPARTICLES
POLLUTION REMEDIATION
CHEMICAL ENGINEERING
ORGANIC-INORGANIC NANOSTRUCTURES

Received
9 May 2013

Accepted
12 August 2013

Published
30 August 2013

Correspondence and requests for materials should be addressed to Q.R.Z. (zhangqr@ysu.edu.cn) or T.F.J. (tfjiao@ysu.edu.cn)

Rationally designed porous polystyrene encapsulated zirconium phosphate nanocomposite for highly efficient fluoride uptake in waters

Qingrui Zhang, Qing Du, Tifeng Jiao, Zhaoxiang Zhang, Sufeng Wang, Qina Sun & Faming Gao

Hebei Key Laboratory of Applied Chemistry, School of Environmental and Chemical Engineering, Yanshan University, Qinhuangdao 066004, PR China.

Fluoride pollution in waters has engulfed worldwide regions and an excess of fluoride intake always causes skeletal fluorosis. Herein, a novel hybrid nanomaterial ZrP-MPN was fabricated for fluoride retention by encapsulating nano-ZrP onto macroporous polystyrene materials modified with quaternary ammonium groups. The as-obtained materials exhibited favorable removal of fluoride ions from aqueous solution in presence of common anions (SO_4^{2-}/NO_3^-/Cl^-) at high contents. Moreover outstanding sorption properties were also detected by involving series of commercial adsorbents (AA/magnetite/GFH/manganese sands) as references. Such satisfactory performances might be ascribed to the structural design of nanocomposite. (1) the $CH_2N^+(CH_3)_3Cl$ groups enhances sorption diffusion and preconcentration in sorbent phase theoretically based on Donnan membrane principle; (2) the embedded ZrP nanoparticles also devotes to the efficient adsorption capacities due to its size-dependent specific properties. Additionally, the exhausted ZrP-MPN could be regenerated readily by alkaline solution. Thus, ZrP-MPN was a promising material for fluoride retention in waters.

The ingestion of excess fluoride in drinking water causes harmful effects such as dental/skeletal fluorosis[1]. Now, millions of humans around worldwide are suffering from severe fluoride pollution, which derives mainly from the dissolution of fluoride-rich rocks and interaction at the solid-water interface. Thus, fluoride pollution is a serious regional problem[2,3]. Recently, inorganic nanoparticles with various morphology i.e. flower-like a-Fe_2O_3[4,5], nest-similar structures of magnesium oxide nanocrystal[6,7], MgAl-CO_3 layered double hydroxides[8] and charge-dependent ZnS[9] etc. have proven to be efficient adsorbents for fluoride or other trace pollutants retention[10–15], owing to the formation of inner-sphere complexation and the specific size-dependent properties. In general, nanosized materials exhibit high surface area and abundant active sites, thus, as expected, the nanoparticles could display outstanding fluoride sorption performances[16]. However, engineering nanoparticles for fluoride remediation are still far from application, because of the limitation of the following issues[17]: (1) nanoparticles always tend to aggregate and greatly weaken the size-dependent sorption efficiencies; (2) difficulty in solid-liquid separation; (3) the ultrafine nanoscale particles are fail to apply in fixed beds or flow through systems, due to excessive pressure drops and flow resistances etc.[18,19].

To debate the bottleneck of nanoparticle engineering, an alternative technology is the development of hybrid nanomaterials by embedding inorganic nanoparticles onto the porous granulated carriers[20,21], such as activated carbon[22–24], zeolite[25], diatomite[26], cellulose[27], alginate[28] and macroporous polymer[29–31]. The resulting nanocomposites present excellent handing and better hydraulic conductivity due to their large particle properties and their porous host matrix, which could also render nanoparticles immobilization within the inner surfaces. Therefore, the exploitation of hybrid nanomaterials is an important strategy for nanoparticle engineering, whereas the poor diffusion kinetics resulting from pore blockage during incorporation process, might be a challenge for field application[32].

Group IVB phosphate, i.e. Zr/Ti/Hf phosphate is an important catalog of inorganic materials and zirconium phosphate (denoted as ZrP), the most representative one, has been widely studied as solid acid catalyst[33], which exhibits excellent chemical stability, extremely insolubility in water, strong acid and organic reagents, fast kinetics and environment- friendly properties. As for its sorption behaviors, in the 1960s, A. Clearfield and G. Alberti

research groups have systematically investigated the fabrication of ZrP with various particle sizes, crystallization, morphology and the preferential sorption of K(I)/Na(I)/LI(I)/Ca(II)/Mg(II)/Ba(II) etc[34]. Recently, some research groups and our previous study demonstrated the nanostructured ZrP displays favorable sorption towards heavy metals and organic compounds retention[35,36]. More recently, mesoporous ZrP particles were synthesized for trace fluoride removal in drinking waters[37]. Unfortunately, ZrP was also obtained as the white ultrafine powders and couldn't be used directly in practice.

Herein, a novel hybrid nanomaterial (ZrP-MPN) was fabricated for fluoride ions retention by anchorage of nano-ZrP onto macroporous polystyrene beads modified with quaternary ammonium groups ($-CH_2N^+(CH_3)_3$). As compared to the conventional carriers, macroporous polystyrene beads as an ideal host matrix exhibit dominant superiority, i.e. the positive-charged quaternary ammonium groups binding to the host materials could present electrostatic interaction towards the target fluoride ions, leading to the enhanced sorption diffusion kinetics and fluoride ions enrichment, prior to sequestration by nano-ZrP, such phenomenon is the so-called "Donnan membrane effect"[38,39]. Recent research also further proved that such polymer encapsulating metal nanoparticles could cause negligible toxic effects on organism in waters[40]. Besides, the excellent chemical stability and non-toxic properties of ZrP particles also render us believe that the hybrid nanomaterial ZrP-MPN is a promising adsorbent towards fluoride retention.

Results

Characterization of the hybrid nanomaterials. The simple schematic structure of the resulting sorbent ZrP-MPN was presented in Figure 1 and the hybrid nanomaterials were characterized by scanning electron microscopy (SEM), transmission electron microscopy (TEM), X-ray diffraction (XRD), thermogravimetric analysis (TGA), and atomic force microscopy (AFM) and nitrogen sorption measurement for pore analysis. As depicted in Figure 2(a–c), the obtained nanocomposites were spherical beads, then the resulting adsorbent was subjected to cutting into half and the inner surface morphologies were described by SEM analysis. The morphological comparisons of the hybrid materials and its matrix indicated that ZrP particles were successful embedded into the inner surface of ZrP-MPN and blocked some cross-linked pores, the corresponding Zr element scanning by SEM-EDS (Figure 2f) further demonstrated the encapsulated ZrP distributed in a ring-like region. Besides, AFM analysis was also performed to obtain new insight toward the impregnated ZrP particles. As shown in Figure 2(d, e, d′ e′), the morphology of the inner surface within MPN exhibited outstanding height differences (vertical height $>$ 1 μm), which indicated the broad macroporous structures, whereas for the hybrid nanomaterial ZrP-MPN, the uniform surface height variations (240–310 nm detected in Figure 2(d′ e′)) suggests the implantation of ZrP nanoparticles blocks some of nanopores. Furthermore, the ZrP amounts of ZrP-MPN (about 24.3% in mass) according to the contents variation before and after loading by ICP analysis also implied the success anchorage of ZrP particles. nitrogen sorption measurement (Table 1) for pore structure analysis further revealed similar appearances and the incorporation of ZrP particles resulted in a significant decrease in pore volume and average pore sizes, which might ascribe to the possible pore blocking during incorporation process. However, it is worth to note that a slightly increase in BET surface areas from 17.0 to 22.3 m^2/g, possibly attributed to the formation of nanosized ZrP particles[32,41,42]. Nanoscale materials usually present larger surface areas and abundant active sites, thus, as expected, the specific areas could offer preferential sorption towards fluoride retention. TEM images (Figure 2g) further proved that the encapsulated ZrP particles were monodispersed nanoparticles with size 20–30 nm. XRD spectrum (Figure 2i) of ZrP-MPN beads illustrated that the embedded ZrP particles were amorphous in nature, note that the mild synthesis conditions might

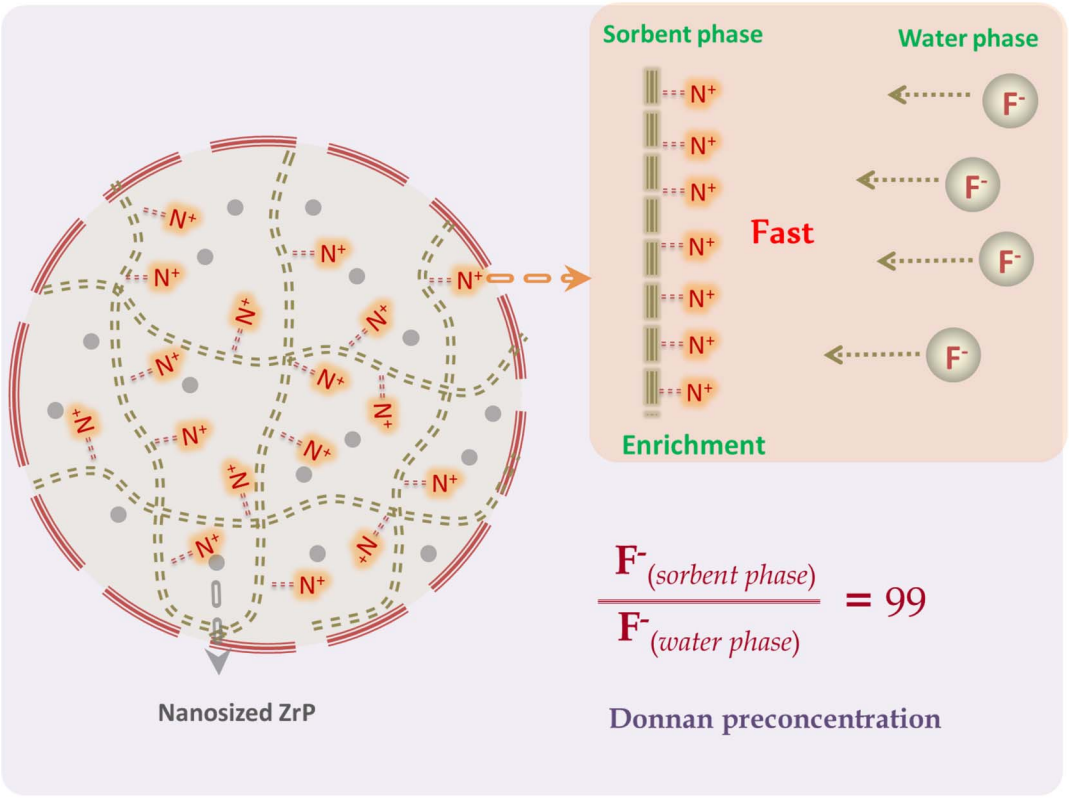

Figure 1 | **The schematic structure of the hybrid nanomaterials ZrP-MPN.**

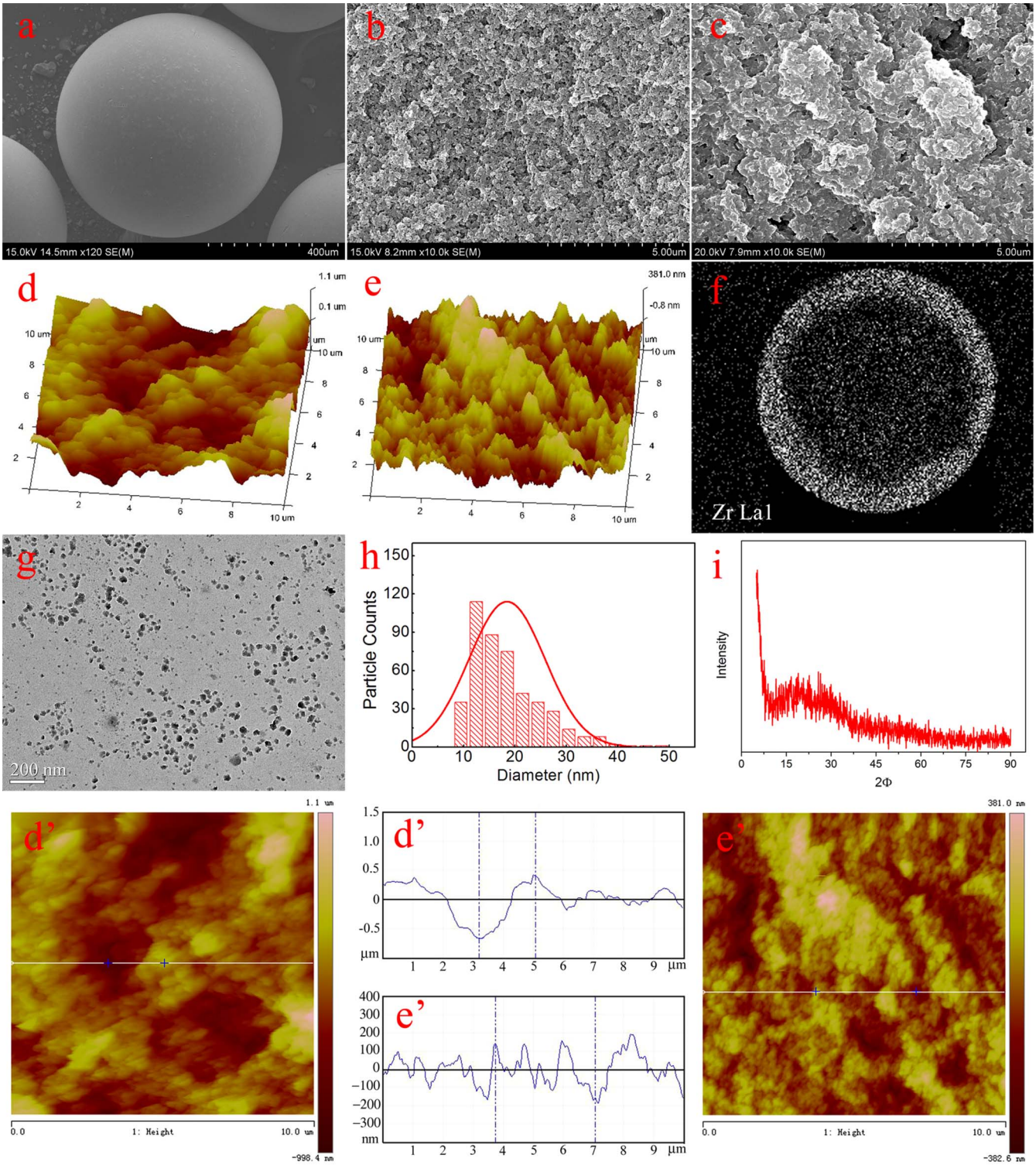

Figure 2 | Characterization of the nanocomposite ZrP-MPN and its host matrix MPN (a) SEM of the spherical bead Zr-MPN; (b) SEM of inner surfaces within the host material MPN; (c) SEM of inner surfaces within Zr-MPN; (d) AFM 3D analysis onto the inner surface of MPN; (e) AFM 3D analysis onto the inner surface of ZrP-MPN; (f) cross-section Zr distribution of ZrP-MPN by SEM-EDS; (g) TEM of Zr-MPS; (h) the encapsulated ZrP nanoparticle size distribution derived from Figure 1-(e); (i) XRD spectrum of ZrP-MPN. (d′) AFM line profile analysis of MPN; (e′) AFM line profile analysis of ZrP-MPN.

more suitable for amorphous ZrP formation, and in fact, the amorphous ZrP might exhibit more favorable sorption performances than the crystal[41]. TGA curves (Figure S1) indicated the hybrid materials exhibit good thermal stability. It is worthy to note that the observed weight loss (16%) below 400°C mainly ascribed to the evaporation of the external water and further increasing the temperatures reduce significant weight loss for the decomposition of polymeric matrix within ZrP-MPN.

Fluoride retention in batch sorption behaviors. To evaluate the sorption properties towards fluoride ions, batch sorption tests were performed by conventional bottle-points methods. Solution pH is

Table 1 | Salient properties of polymeric host materials and the hybrid materials

Designation	Host materials MPN	Hybrid materials ZrP-MPN
Matrix structure	Polystyrene	Polystyrene
Surface groups	$-CH_2N^+(CH_3)_3Cl$	$-CH_2N^+(CH_3)_3Cl$
Contents of groups (meq/g)	3.1	NA
BET surface area (m^2/g)	17.0	22.3
Average pore diameter (nm)	15.2	12.3
Pore volume (cm^3/g)	0.065	0.061
ZrP content (mass%)	0	24.3%

one of the most important parameters, which directly influences the adsorption behaviors of fluoride ions. Herein, the effects of solution pH on fluoride retention were investigated and the results were shown in Figure 3. It was observed that the fluoride uptake onto the resulting material ZrP-MPN was a pH-dependent process and the optimal sorption condition was pHs = 3.0. Further increase or decrease in pH values could bring about the unfavorable fluoride ions removal. In general, the hybrid nanomaterial contains two different sorption sites, i.e. the quaternary ammonium ($-CH2N^+(CH_3)_3Cl$) binding to the host matrix and the embedded ZrP nanoparticles. The detailed reaction mechanisms were presented in Figure 4[37,42].

It is shown that fluoride uptake onto quaternary ammonium groups was mainly driven by electrostatic adsorption. Whereas, as for ZrP, low pHs favored protonation of hydroxyl groups covalent zirconium atoms within the nanoparticle interfaces, thus large number of positively charged sites promoted the negative fluoride retentions. Moreover, as observed in pH = 0.6–3.0, excess H^+ ions addition could result in the formation of neutral HF, which was not conducive to the sorption efficiencies; furthermore, the higher pHs involved in deprotonation of OH_2^+ and the ZrP surface becomes negatively charged ($Zr\text{-}O^-$), thus, the repulsion forces were enhanced, and the removal of fluoride ions drops. Besides, we also examined the Zr elements release at various pH value, the negligible loss of zirconium suggested the well sorption stability onto the nanocomposite ZrP-MPN[44,45].

It is well known that the common ions such as SO_4^{2-}, NO_3^- and Cl^- are ubiquitous in drinking water or wastewaters. Thus, the competitive sorption towards fluoride ions was performed to elucidate the outstanding selectivity onto ZrP-MPN and its matrix MPN was also involved for comparison. As depicted in Figure 5(a–c), it can be seen that the defluoridation efficiency of both ZrP-MPN and MPN exhibit negative trends due to common anions interference. Whereas, by contrast to the matrix material MPN, the obtained nanomaterial ZrP-MPN still remained outstanding sorption selectivity. Of particular note that the fluoride removal efficiency onto ZrP-MPN was slightly influenced by the added competing anions even at 30 times higher than the target fluoride ions, whereas that onto MPN, the serious competition results in dramatically sorption suppression and the removal efficiencies even approach near to zero. Such distinguished performances might mainly attribute to the different sorption sites and interaction mechanism towards fluoride uptake. As above discussed, the quaternary ammonium groups ($-CH_2N^+(CH_3)_3Cl$) within the matrix exhibit nonspecific sorption through electrostatic interaction, thus the high contents of common anions might lead to serious sorption competition and ignorable removal rates obtained. Whereas, in view of the nanocomposite ZrP-MPN, the encapsulated ZrP nanoparticles could exhibit strongly metal-ligand complexation with fluoride ions in aqueous and increase the sorption selectivity. Moreover, as compared to the commercial adsorbents for defluoridation[12,43,46] (i.e. activated aluminum (AA), magnetite, granular ferric hydroxides (GFH), and manganese sands), ZrP-MPN also showed preferential sorption ability and all the satisfactory performances further prove that the nanocomposite ZrP-MPN is a potential nanoscale sorbent for defluoridation.

Sorption kinetics. In general, relating to hybrid nanomaterials fabrication, the nanosized ZrP entrapment might result in pore

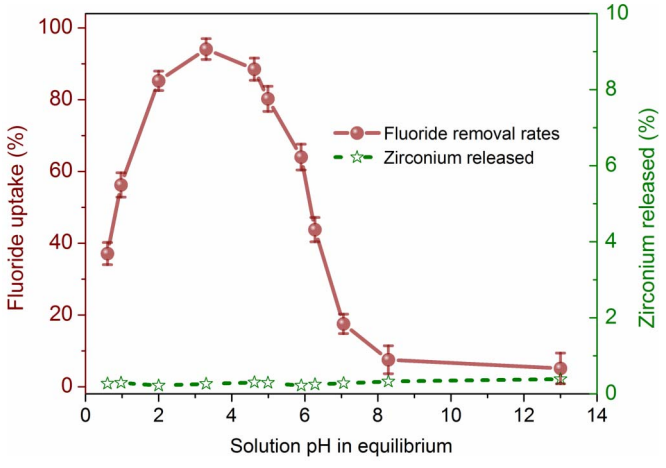

Figure 3 | Effect of solution pH and corresponding Zr release on the uptake of fluoride ions onto ZrP-MPN. (conditions: 1 g/L ZrP-MPN, initial fluoride contents: 10 mg/L, 50 mL solution at 298 K).

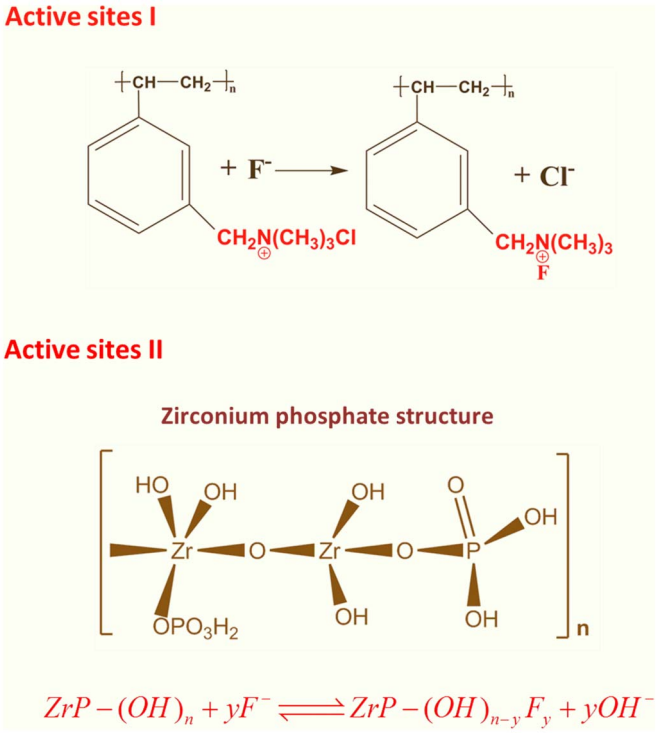

Figure 4 | Sorption mechanism towards fluoride ions of the hybrid nanomaterials ZrP-MPN.

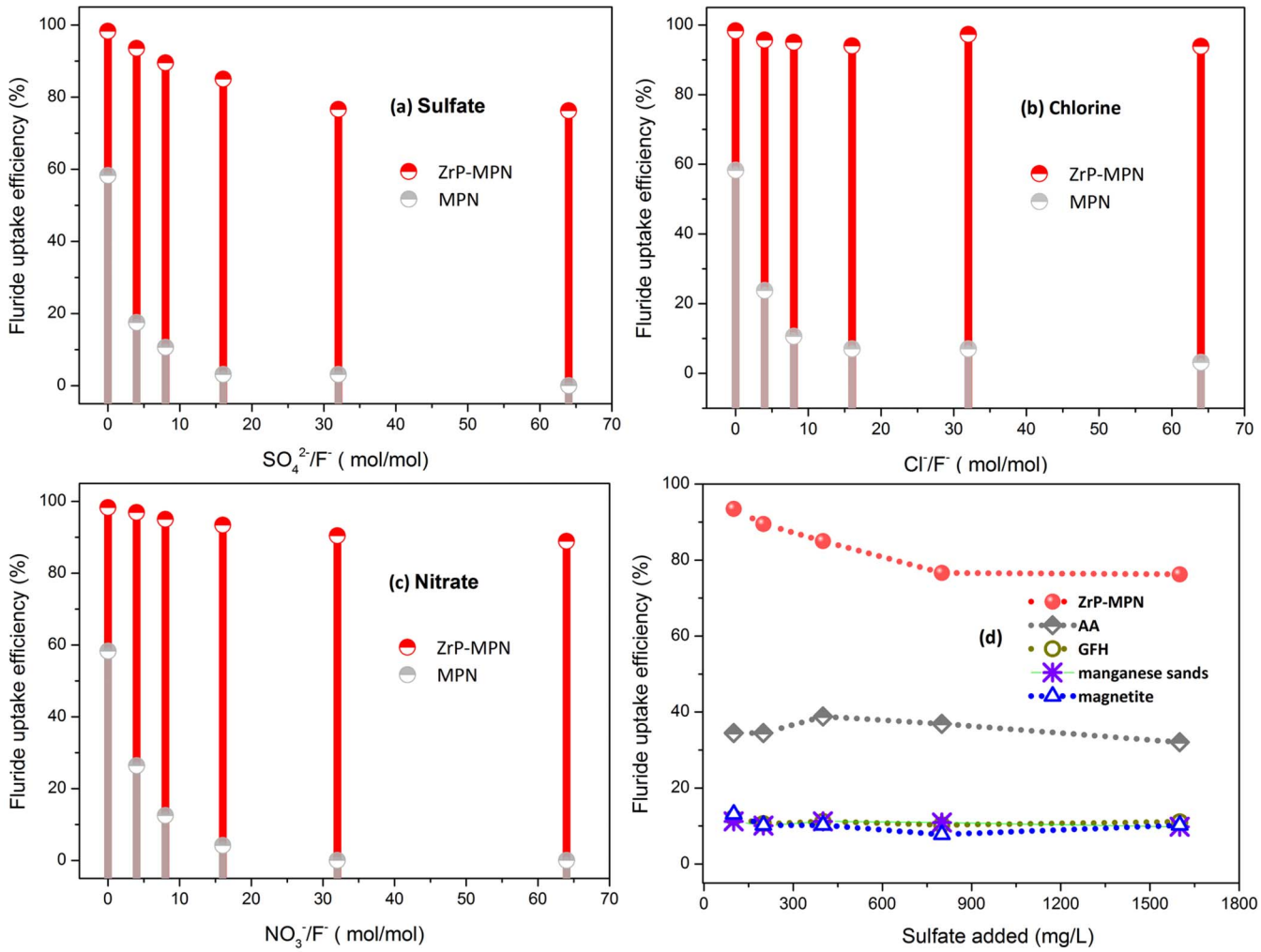

Figure 5 | Competative effect on uptake of fluoride ions onto ZrP-MPN and its host material MPN for (a–c). (a) sulfate interfere; (b) chlorine interfere; (c) nitrate interfere; (d) comparsion of sorption performances with the common used adsorbent for defluoridation (conditions: 0.1 g adsorbent, initial F^- = 10 mg/L, pH = 5.5-6.3; 50 mL solution at 298 K).

blocking, which could bring out the inaccessibility for fluoride removal due to the poor kinetic diffusion. In this section, sorption kinetics experiments were examined and the results were presented in Figure 6. Observably, it could be detected that fluoride uptake onto both ZrP-MPN and MPN showed rapid sorption processes and the equilibriums were achieved within 30 min. The fast sorption kinetics of ZrP-MPN suggests the serious pore clogging (detected in Nitrogen sorption measurements) in encapsulation process didn't cause significant inhibition toward sorption diffusion of fluoride ions.

Such interesting phenomenon might associate with the positive-charged quaternary ammonium groups binding to the surface of polystyrene matrix which could lead to sorption permeation enhancement and preconcentration towards F^- retention. such structure functional design was derived from the principle of "Donnan membrane effects". Afterward, the pseudo-first-order and pseudo-second-order kinetic models were employed to describe the sorption process as follows:

The pseudo-first-order model:

$$\log(q_e - q_t) = \log q_e - \frac{k_1}{2.303}t \quad (1)$$

The pseudo-second-order model:

$$\frac{t}{q_t} = \frac{1}{k_2 q_e^2} + \frac{t}{q_e} \quad (2)$$

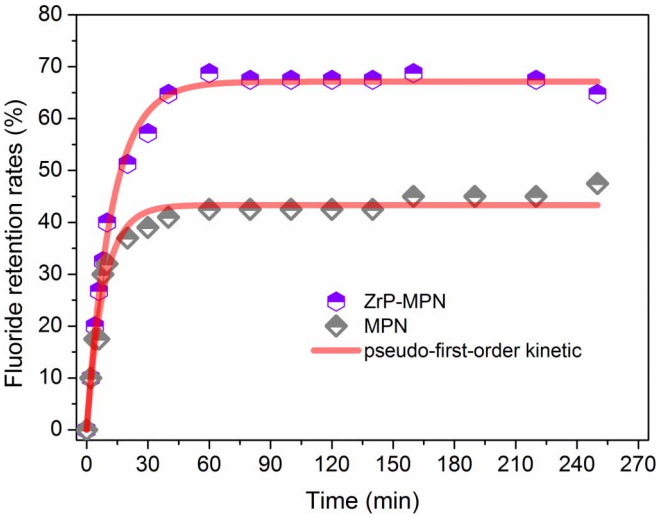

Figure 6 | **Adsorption kinetics of fluoride ions onto ZrP-MPN and MPN at 298 K. (0.50 g adsorbents and 1000 mL solution containing F^- = 10 mg/L in the study).**

Where q_e and q_t present the sorption capacities in equilibrium and time t respectively, and k_1 and k_2 are the sorption kinetic constants. Relative kinetic data have been shown in Table S1. Obviously, the sorption onto ZrP-MPN could be well described by the pseudo-first-order model as compared to the pseudo-second-order one(Figure S2), due to the high correlation coefficient (>0.990), and the calculated qe value (6.60 mg/g) was also close to the experimental data (6.65 mg/g).

Fixed-bed column tests for engineering nanocomposites. Figure 7 illustrates an effluent history of high-speed column system packed with ZrP-MPN for a feeding stimulated drinking solution containing fluoride ions and the water composition data were detected and obtained from Dujiazhuang village, Ping Yao, Shanxi Province. The host material MPN was also introduced for comparison. As depicted in Figure 6, it could be seen that the fluoride uptake broke through quickly onto MPN, because of its poor sorption selectivity and serious competition effects of common coexist anions with the effective treatment volume about 25 bed volumes before significant leakage. By contrast, ZrP-MPN displayed more efficient sorption performances with treatment time 19 hours and 380 BV purified waters and the corresponding working sorption capacities approach to around 1.6 mg/g (maximum: 6.6 mg/g). Moreover, the efficient adsorption of fluoride also lead to the low effluent contents (<0.1 mg/L.), which was even an order of magnitude lower than the drinking water standards recommended by WHO[47]. Such satisfactory removal performances further demonstrated the favorable sorption and specific affinities towards fluoride ions sequestration by the resulting nanomaterials.

Regeneration of exhausted ZrP-MPN beads could be achieved in a column system by using binary mixtures (5%NaOH + 5%NaCl), and the results (Figure 7) suggested that the used nanomaterials could be effectively extracted in 5 bed volumes with the desorption efficiency higher than 99%. Note that after regeneration, the packed ZrP-MPN column was subjected to rinsing with waters and 3% NaCl solution till pH < 7 to ensure the same solution chemistry in the next sorption cycles.

Discussion

In present study, a novel hybrid nanomaterial was fabricated by encapsulating nanosized ZrP onto the polymeric porous matrix modified with quaternary ammonium groups. In the competing tests (Figure 4) section, the presence of quaternary ammonium groups seems to be powerless, because of the nonspecific electrostatic interaction. In fact, the design of surface groups mediation was important and a must and the positive-charged groups ($-CH_2N^+(CH_3)_3Cl$) exhibit enhanced sorption diffusion and enrichment towards F^- ions, prior to the retention of nanosized ZrP particles. Such an excellent phenomenon is the so-called "Donnan membrane effect" which always leads to the large sorption capacities and low effluent contents towards target pollutants.

Specifically, the detailed schematic diagram for mechanism explanation was presented in Figure 8. According to the Donnan principles, we assumes that the sorptive system was separated by a diffusion membrane, and the left phase was adsorbent and the right assigned to water phase. Thus, as for the common hybrid materials (carrier:GAC/zeolite/polymer), 0.01 M sodium fluoride passes through the assumed membrane and approach to equilibrium with equation as follows

$$\frac{Na^+_{(water)}}{Na^+_{(adsorbent)}} = \frac{F^-_{(adsorbent)}}{F^-_{(water)}} = 1 \qquad (3)$$

On the basis of the above equation, the fluoride ions in aqueous were divided equally into sorbent and water phases. In view of our present study, The positive quaternary ammonium groups within ZrP-MPN were immobilized and couldn't be moved through the diffusion membrane. Thus, in the left phase, the extra charges would greatly attract the target fluoride ions to the sorbent surface. In the same conditions above, nearly 100 folders enrichment achieved at

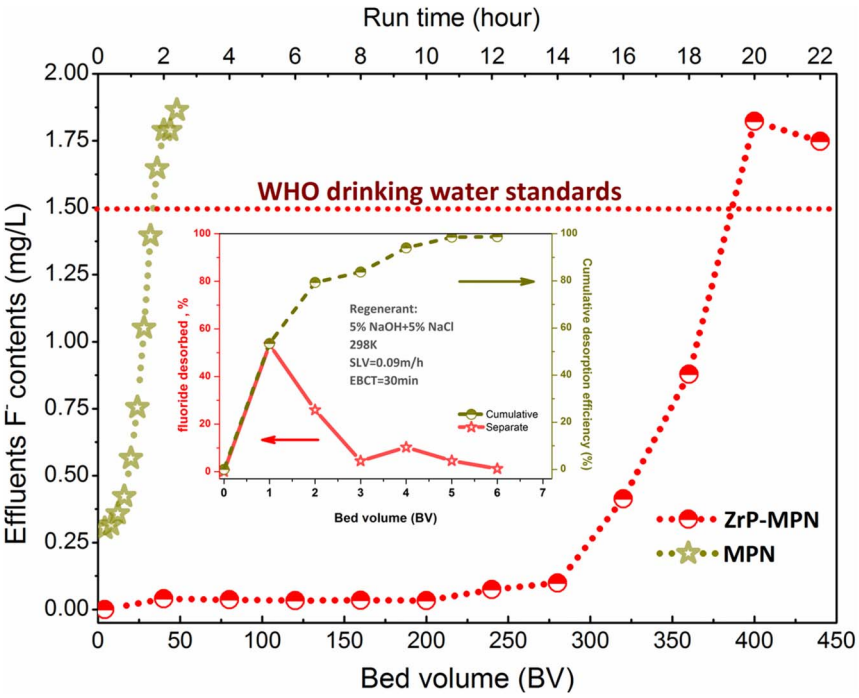

Figure 7 | Comparison of breakthrough curves of fluoride uptake onto ZrP-MPN and MPN with separate fixed-bed column runs at 298 K. (adsorption conditions: inffluent F^- = 2 mg/L, SO_4^{2-} = 20 mg/L, Cl^- = 100 mg/L, NO_3^- = 50 mg/L, pH = 6.2–6.5, SLV = 1.0 m/h, EBCT = 3 min; desorption: 5%NaOH + 5%NaCl mixtures, 298 K, SLV = 0.05 m/h and EBCT = 60 min).

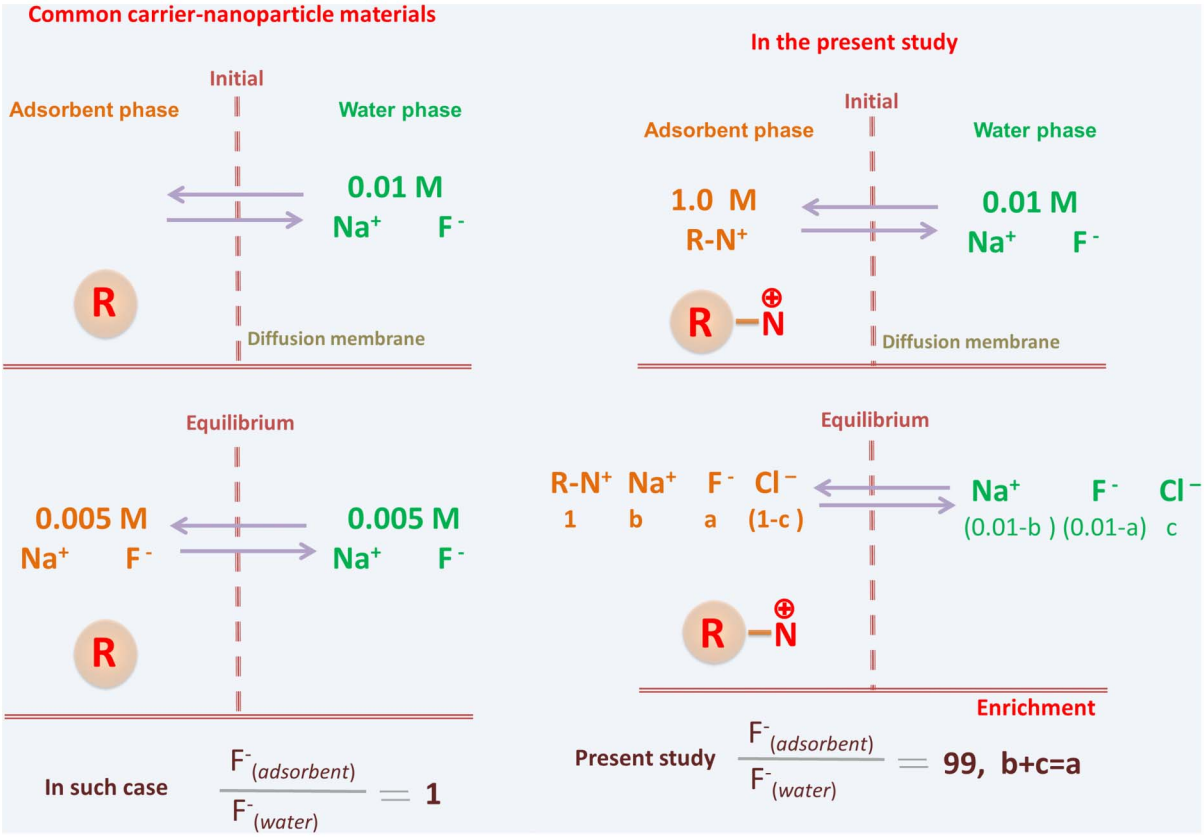

Figure 8 | The design mechanism of the hybrid nanomaterial ZrP-MPN according to Donnan membrane principle in the present study.

equilibrium in sorbent phase and got a corresponding low contents of fluoride ions in the water phase, which was in agreement with the results of column tests (Figure 6) and the detailed formula as follows:

$$\frac{Na^{+}_{(water)}}{Na^{+}_{(adsorbent)}} = \frac{Cl^{-}_{(adsorbent)}}{Cl^{-}_{(water)}} = \frac{F^{-}_{(adsorbent)}}{F^{-}_{(water)}} = 99 \qquad (4)$$

Theoretically, the equations 3 and 4 give us an interesting guideline towards hybrid nanomaterial fabrication based on the Donnan enrichment principles. i.e. if the ZrP nanoparticles were incorporated onto the carriers containing fixed positive-charged N^{+} groups, the target fluoride ions will assemble in the sorbent regions and the removal performances will be greatly enhanced. Thus, the design of hybrid nanomaterials containing fixed-charge groups was necessary and rational.

As for the characterization of ZrP-MPN, we can see that the Zr element mainly distributed in the outer-ring areas by SEM-EDS analysis. Such phenomenon was interesting and understandable, the presences of positive charged ammonium groups will prevent the Zr(IV) salts diffusion into the center areas. Besides, the ring-like distribution of zirconium elements also suggests that the incorporation of ZrP nanoparticles was a gradual process and the pore blocking in preparation could be also an important cause of the ring-like areas formation. In the XRD spectrum, the implanted ZrP particles were mainly presented as amorphous in nature. Note that the species of amorphous pattern might exhibit more favorable fluoride sequestration than the crystals. Similar results were also observed and preliminary proved in our previous study for heavy metal removal by ZrP crystalline and the crystal lattice might be important structural barriers for pollutants diffusion and permeation.

The effects of solution pH on fluoride uptake were performed and the encapsulated ZrP nanoparticles showed excellent stability at wide pHs regions which could mainly ascribe to the unique chains structure of matrix pores. The polymeric cross-linked chains within matrix could exhibit net-like roles and its compact intersection structure could prevent the loaded ZrP nanoparticles from leaching into the surrounding solution. Besides, the well stability and negligible sorption capacities towards fluoride ions at pH $>$ 8 also indicate the reliable regeneration in alkaline solutions.

For the hybrid nanomaterials engineering in fixed-bed column tests, ZrP-MPN beads presented good performance with trace fluoride ion contents in effluent solution. The remarkable behaviors might be the joint actions of Donnan membrane enrichment and nano-ZrP size-dependent efficiency. The resulting low fluoride contents below 0.1 mg/L might be credited with the positive-charged groups diffusion enhancement, while the presence of nanosized ZrP particles mainly favored the large sorption capacities and performances.

In summary, nano-ZrP supported by macroporous polystyrene beads with quaternary ammonium groups modification is fabricated based on Donnan membrane principles for efficient fluoride ion removal in waters. As compared to the host materials MPN and commercial used adsorbents, ZrP-MPN exhibits more preferential adsorption towards fluoride ions in presence of common anions at high levels. Fixed-bed column tests further proved the excellent performances and low fluoride concentration in effluents, which mainly attributed to the potential Donnan membrane enrichment onto the fixed-charge groups as well as the encapsulated ZrP nanoparticles of specific interaction with fluoride ions. Furthermore, the exhausted ZrP-MPN is amenable to efficient regeneration by alkaline brine solution. All the experimental results indicated that the hybrid nanomaterial was a promising adsorbent for trace fluoride ions retention in waters.

Methods

Fabrication of the hybrid nanomaterials ZrP-MPN. In the present study, all the chemical agents were analytic grade and used without further purification. The synthesis of polystyrene-based ZrP nanocomposites was carried out in two important

steps: (1) Preparation of the host materials MPN; (2) ZrP nanoparticles encapsulation within MPN.

Preparation of the host materials MPN. The synthesis of host material was performed by using conventional suspension polymerization. Briefly, 0.5 g of benzoyl peroxide was dissolved in a mixed solution of 82.5 g styrene and 17.5 g of divinylbenzene (content 40%), liquid paraffin was also added for pore structure. Then, the above mixture(oil phase) were dropped into 400 mL distilled water containing 0.5% polyvinyl alcohol (dispersing agent) in a three-necks flask. The mixture solution was subjected to stirring with the temperature of 45°C for 3 hours, afterward, the temperature was raised to 90°C and boiled 6 h. Meanwhile, the reaction in oil phase finished and obtained white uniform beads. Finally the beads were immersed in a soxhlet extractor for removal of extra paraffin to achieve the formation of porous structures and obtain the macroporous polystyrene beads (MP).

MP beads were used as starting materials for surface functional group modification. 40 mL of MP beads were introduced into 200 mL chloromethyl ether, and 20 g anhydrous zinc chloride was selected as catalyst. The above mixtures were stirred at 40°C for 12 h, then the beads were filtrated and washed in pure water and ethanol solutions. Thus, an intermediate product was prepared with -CH_2Cl functionalization (MPC). To prepare the target carriers containing quaternary ammonium groups (-$CH_2N^+(CH_3)_3Cl$), 20 mL MPC was subjected to amination reaction by adding 200 mL of trimethylamine solution at 318 K for 24 h. Finally, the residue trimethylamine was decanted, and the solid beads were washed with 200 mL of ethanol and 1,000 mL of deionized water to get the resulting matrix of MPN.

ZrP nanoparticles encapsulation within MPN. 20.0 g host matrix MPN beads were put into 150 mL $ZrOCl_2$-HCl binary solutions and the mixture was stirred in water bath system at 303 K for 7 h to ensure transport of the amount of zirconium salts onto the inner porous of MPN. In the next step, the above resulting polymeric beads were filtered and gradually added into 1000 mL 30% H_3PO_4 solution at room temperatures reaction for 8 h, thus, the Zr(IV) compounds were precipitated as $Zr(HPO_4)_2$ onto the inner surface of MPN. Finally, the obtained materials were subjected to washing with ultrapure water till pH = 5–6 and heat treating at 333 K for 6 h to get the hybrid nanocomposite (ZrP-MPN).

Batch sorption experiments. Batch sorption tests were carried out by traditional bottle-point methods, and the detailed experimental methods were developed by solution pH effects on adsorption, competing experiments and kinetics tests.

Effects of solution pH. In the present study, 0.05 g ZrP-MPN beads were introduced into 150 mL plastic bottles containing 50 mL 10 mg/L F^- with different pH (1–14) solutions adjusted by HNO_3 (1%) or NaOH (1%) throughout the experiments. The bottles were then transferred into incubator shaker at desired temperature for 24 h to ensure to reach sorption equilibrium. Finally, the solutions were subjected to filtering and the equilibrium solution pH and corresponding contents were determined.

Competing sorption. To start the experiments, 0.1 g materials (ZrP-MPN, MPN, activated alumina, magnetite, granular ferric oxides, and manganese sands) were added into 50-ml solution containing known contents fluoride solution and the common anions SO_4^{2-}/NO_3^-/Cl^- were also introduced if necessary. The plastic flasks were then transferred into a G-25 model incubator shaker with thermostat and shaken under 200 rpm for 24 h, and then the equilibrium fluoride contents were assayed.

Kinetic experiments. Sorption kinetics tests were performed by sampling 0.5 mL-solution at various times by using a liquid-transferring gun and the initial solution volume was 1000 mL containing a known concentration of fluoride ions and 0.5 g ZrP-MPN beads, Kinetic data were calculated by detecting the sample contents at various times.

Fixed-bed column tests. High-speed column tests were carried out in a small plexiglass column (14 mm diameter and 150 mm length) equipped with water bath equipment and 5.0 mL of ZrP-MPN and MPN were selected as adsorbents packed in separated columns. A Lange-580 pump (China) was used to ensure a constant flow rate of feeding solution. A simulated drinking water derived from assaying data of Dujiazhuang village, Shanxi province containing a certain contents common ions (SO_4^{2-}, NO_3^-, Cl^-, Na^+, Ca^{2+}, Mg^{2+}, F^- etc.) was prepared as feeding solution for fluoride contaminated waters evaluation and an automatic fraction collector(SBA-100 Huxi) was used for collecting the effluent samples. The column experiments were performed in high-speed hydrodynamic conditions: the superficial liquid velocity (SLV) and the empty bed contact time (EBCT) were equal to 1 m/h and 3 min, respectively.

Characterization. The Concentration of fluoride in the solution, before and after adsorption, was determined using ion selective electrode (Orion 720 A^+ Ion analyzer) and zirconium contents were assayed by inductively coupled plasma (ICP) (JA-1100, Jarrell-Ash). The images of the encapsulated ZrP particles were taken on a Hitachi S-4800 field emission scanning electron microscopy coupled with energy dispersive spectroscopy with the accelerating voltage of 5–15 kV; TEM images were recorded using high-resolution transmission electron microscopy (HRTEM, JEM2010) equipped with a Gatan CCD camera working at accelerating voltage of 200 kV. The crystal morphology of entrapped ZrP nanoparticles were characterized by X-ray diffraction (XRD) using an XTRA X-ray diffractometer (Switzerland) and Cu Kα radiation (λ = 1.5418 Å) with a scan rate of 0.02° s^{-1}; AFM images were taken using tapping mode (Nanoscope III a Multimode system, Digital Instruments, Santa Barbara, CA) with silicon nitride cantilever probes. Nitrogen sorption measurements were performed at 77 K to determine the surface area and pore size distribution based on BJH model by using micrometrics ASAP 2020 (U.S.). The thermogravimetric analysis (TGA/DSC) of Perkin-Elmer was carried out to evaluate the stabilities of the samples as the function of temperature in nitrogen atmosphere under a flow of 30 mL/min and heating rate of 10°C/min.

1. Fagin, D. Second thoughts about fluoride. *Sci. Am.* **298**, 74–81 (2008).
2. Mohapatra, M., Anand, S., Mishra, B. K., Giles, D. E. & Singh, P. Review of fluoride removal from drinking water. *J. Environ. Manage.* **91**(1), 67–77 (2009).
3. Meenakshi & Maheshwari, R. C. Fluoride in drinking water and its removal. *J. Hazard. Mater.* **137**(1), 456–463 (2006).
4. Zhong, L. S. *et al.* Self-assembled 3D flowerlike iron oxide nanostructures and their application in water treatment. *Adv. Mater.* **18**(18), 2426–2431 (2006).
5. Cao, C. Y. *et al.* Low-cost synthesis of flowerlike alpha-Fe_2O_3 nanostructures for heavy metal ion removal: adsorption property and mechanism. *Langmuir* **28**(9), 4573–4579 (2012).
6. Cao, C.-Y., Qu, J., Wei, F., Liu, H. & Song, W.-G. Superb adsorption capacity and mechanism of flowerlike magnesium oxide nanostructures for lead and cadmium ions. *ACS Appl. Mater. Interfaces* **4**(8), 4283–4287 (2012).
7. Yu, X. Y. *et al.* Porous hierarchically micro-/nanostructured MgO: morphology control and their excellent performance in As(III) and As(V) removal. *J. Phys. Chem. C* **115**(45), 22242–22250 (2011).
8. Lv, L., He, J., Wei, M., Evans, D. & Zhou, Z. Treatment of high fluoride concentration water by MgAl-CO_3 layered double hydroxides: Kinetic and equilibrium studies. *Water Res.* **41**(7), 1534–1542 (2007).
9. Wang, Y. *et al.* Tunable surface charge of ZnS:Cu nano-adsorbent induced the selective preconcentration of cationic dyes from wastewater. *Nanoscale* **4**(12), 3665–3668 (2012).
10. Mohapatra, M. *et al.* Facile synthesis of additive-assisted nano goethite powder and its application for fluoride remediation. *J. Nanopart. Res.* **12**(2), 681–686 (2010).
11. Sternitzke, V. *et al.* Uptake of fluoride from aqueous solution on nano-sized hydroxyapatite: Examination of a fluoridated surface layer. *Environ. Sci. Technol.* **46**(2), 802–809 (2012).
12. Jagtap, S., Yenkie, M. K., Labhsetwar, N. & Rayalu, S. Fluoride in drinking water and defluoridation of water. *Chem. Rev.* **112**(4), 2454–2466 (2012).
13. Wang, X., Cai, W., Lin, Y., Wang, G. & Liang, C. Mass production of micro/nanostructured porous ZnO plates and their strong structurally enhanced and selective adsorption performance for environmental remediation. *J. Mater. Chem.* **20**(39), 8582–8590 (2010).
14. Wang, J. Q. *et al.* Excellent capability in degrading azo dyes by MgZn-based metallic glass powders. *Sci. Rep.* **2**, 1–6 (2012).
15. Lee, K., Park, S. W., Ko, M. J., Kim, K. & Park, N.-G. Selective positioning of organic dyes in a mesoporous inorganic oxide film. *Nat. Mater.* **8**, 665–671 (2009).
16. Yavuz, C. T. *et al.* Low-field magnetic separation of monodisperse Fe_3O_4 nanocrystals. *Science* **314**(5801), 964–967 (2006).
17. Ali, I. New Generation adsorbents for water treatment. *Chem. Rev.* **112**(10), 5073–5091 (2012).
18. Zhang, Q. *et al.* Selective sorption of lead, cadmium and zinc ions by a polymeric cation exchanger containing nano-$Zr(HPO_3S)_2$. *Environ. Sci. Technol.* **42**(11), 4140–4145 (2008).
19. Jiang, Z. *et al.* Nitrate reduction using nanosized zero-valent iron supported by polystyrene resins: Role of surface functional groups. *Water Res.* **45**(6), 2191–2198 (2011).
20. Chen, N. *et al.* Studies on fluoride adsorption of iron-impregnated granular ceramics from aqueous solution. *Mater. Chem. Phys.* **125**(1–2), 293–298 (2011).
21. Sivasankar, V., Ramachandramoorthy, T. & Chandramohan, A. Fluoride removal from water using activated and MnO2-coated Tamarind Fruit (Tamarindus indica) shell: Batch and column studies. *J. Hazard. Mater.* **177**(1–3), 719–729 (2010).
22. Geng, Z. *et al.* Highly efficient dye adsorption and removal: a functional hybrid of reduced graphene oxide-Fe_3O_4 nanoparticles as an easily regenerative adsorbent. *J. Mater. Chem.* **22**(8), 3527–3535 (2012).
23. Bleyl, S., Kopinke, F.-D. & Mackenzie, K. Carbo-iron®–synthesis and stabilization of Fe(0)-doped colloidal activated carbon for in situ groundwater treatment. *Chem. Eng. J.* **191**(0), 588–595 (2012).
24. Tchomgui-Kamga, E. *et al.* Preparation and characterization of charcoals that contain dispersed aluminum oxide as adsorbents for removal of fluoride from drinking water. *Carbon* **48**(2), 333–343 (2010).
25. Yin, M., Li, Z., Liu, Z., Yang, X. & Ren, J. Magnetic self-assembled zeolite clusters for sensitive detection and rapid removal of mercury(II). *ACS Appl. Mater. Interfaces* **4**(1), 431–437 (2012).
26. Caliskan, N., Kul, A. R., Alkan, S., Sogut, E. G. & Alacabey, İ. Adsorption of zinc(II) on diatomite and manganese-oxide-modified diatomite: A kinetic and equilibrium study. *J. Hazard. Mater.* **193**, 27–36 (2011).

27. Liu, Z. *et al*. Magnetic cellulose-chitosan hydrogels prepared from ionic liquids as reusable adsorbent for removal of heavy metal ions. *Chem. Commun.* **48**(59), 7350–7352 (2012).
28. Swaina, S. K., Patnaik, T., Patnaik, P. C., Jha, U. & Dey, R. K. Development of new alginate entrapped Fe(III)–Zr(IV) binary mixed oxide for removal of fluoride from water bodies. *Chem. Eng. J.* **215–216**, 763–771 (2013).
29. Solangi, I. B., Memon, S. & Bhanger, M. I. An excellent fluoride sorption behavior of modified amberlite resin. *J. Hazard. Mater.* **176**(1–3), 186–192 (2010).
30. Kumar, V. *et al*. Development of bi-metal doped micro-and nano multi-functional polymeric adsorbents for the removal of fluoride and arsenic(V) from wastewater. *Desalination* **282**, 27–38 (2011).
31. Samatya, S., Mizuki, H., Ito, Y., Kawakita, H. & Uezu, K. The effect of polystyrene as a porogen on the fluoride ion adsorption of Zr(IV) surface-immobilized resin. *React. Funct. Polym.* **70**(1), 63–68 (2010).
32. Zhang, Q. *et al*. New insights into nanocomposite adsorbents for water treatment: A case study of polystyrene-supported zirconium phosphate nanoparticles for lead removal. *J. Nanopart. Res.* **13**(10), 5355–5364 (2011).
33. Asghari, F. S. & Yoshida, H. Dehydration of fructose to 5-hydroxymethylfurfural in sub-critical water over heterogeneous zirconium phosphate catalysts. *Carbohydr. Res.* **341**(14), 2379–2387 (2006).
34. Vivani, R., Alberti, G., Costantino, F. & Nocchetti, M. New advances in zirconium phosphate and phosphonate chemistry: Structural archetypes. *Micro. Meso. Mater.* **107**(1–2), 58–70 (2008).
35. Pan, B. C. *et al*. Selective heavy metals removal from waters by amorphous zirconium phosphate: Behavior and mechanism. *Water Res.* **41**(14), 3103–3111 (2007).
36. Wang, L. *et al*. Stable Organic–inorganic hybrid of polyaniline/α-zirconium phosphate for efficient removal of organic pollutants in water environment. *ACS Appl. Mater. Interfaces* **4**(5), 2686–2692 (2012).
37. Swain, S. K. *et al*. Kinetics, equilibrium and thermodynamic aspects of removal of fluoride from drinking water using meso-structured zirconium phosphate. *Chem. Eng. J.* **171**(3), 1218–1226 (2011).
38. Sarkar, S., SenGupta, A. K. & Prakash, P. The donnan membrane principle: Opportunities for sustainable engineered processes and materials. *Environ. Sci. Technol.* **44**(4), 1161–1166 (2010).
39. Su, Q. *et al*. Fabrication of polymer-supported nanosized hydrous manganese dioxide (HMO) for enhanced lead removal from waters. *Sci. Total Environ.* **407**(21), 5471–5477 (2009).
40. Felix, L. C., Ortega, V. A., Ede, J. D. & Goss, G. G. Physicochemical characteristics of polymer-coated metal-oxide nanoparticles and their toxicological effects on zebrafish (Danio rerio) development. *Environ. Sci. Technol.* **47**(12), 6589–6596 (2013).
41. Jiang, P., Pan, B., Zhang, W. & Zhang, Q. A comparative study on lead sorption by amorphous and crystalline zirconium phosphates. Colloids Surf. *A* **322**(1–3), 108–112 (2008).
42. Zhang, Q. R. *et al*. Sorption enhancement of lead ions from water by surface charged polystyrene-supported nano-zirconium oxide composites. *Environ. Sci. Technol.* **47**(12), 6536–6544 (2013).
43. Pan, B. C., Xu, J. S., Wu, B., Li, Z. G. & Liu, X. T. Enhanced removal of fluoride by polystyrene anion exchanger supported hydrous zirconium oxide nanoparticles. *Environ. Sci. Technol.* In press.
44. Standards for drinking water quality. Organization, Ministry of Environmental Protection of the People's Republic of China, Beijing, (1996).
45. Integrated wastewater discharge standard. Organization, Ministry of the People's Republic of China, Beijing, (2007).
46. Kumar, E. *et al*. Defluoridation from aqueous solutions by granular ferric hydroxide (GFH). *Water Res.* **43**(2), 490–498(2008).
47. Guidelines for drinking-water quality. In 3rd ed.; Organization, World Health Organization Geneva, (2008).

Acknowledgments

We greatly acknowledge the financial support from the National Natural Science Foundation of China (grant NO.21207112, 21301151, 41271102), the Natural Science Foundation of Hebei Province (No. B2012203060, B2013203317, B2013203108), the China Postdoctoral Science Foundation (No. 2011M500540, 2012M510770, 2013T60265), the Science Foundation for the Excellent Youth Scholars from Universities and Colleges of Hebei Province (No. Y2011113), the Scientific Research Foundation for Returned Overseas Chinese Scholars of Hebei Province (No. 2011052) . We also thank Dr. Xianwei Liu (Arizona State University) and Xinqing Chen (UST HK) for their insightful comments and English improvement during the preparation of the manuscript.

Author contributions

Z.Q.R. and J.T. planned the project and data analysis. D.Q. and Z.Z. carried out the experimental works; S.Q., W.S. and G. F. prepared all the figures, all the authors discussed the data, interpreted the results and jointly wrote the paper.

Additional information

Supplementary information accompanies this paper at http://www.nature.com/scientificreports

Competing financial interests: The authors declare no competing financial interests.

How to cite this article: Zhang, Q.R. *et al*. Rationally designed porous polystyrene encapsulated zirconium phosphate nanocomposite for highly efficient fluoride uptake in waters. *Sci. Rep.* **3**, 2551; DOI:10.1038/srep02551 (2013).